



# Roles of water and dissolved oxygen in photocatalytic generation of free OH radicals in aqueous TiO<sub>2</sub> suspensions: An isotope labeling study

A.O. Kondrakov<sup>a,b,c,\*</sup>, A.N. Ignatev<sup>a,b</sup>, V.V. Lunin<sup>b</sup>, F.H. Frimmel<sup>a</sup>, S. Bräse<sup>c</sup>, H. Horn<sup>a,d</sup>

<sup>a</sup> Chair of Water Chemistry and Water Technology, Karlsruhe Institute of Technology, Engler-Bunte-Ring 1, Karlsruhe 76131, Germany

<sup>b</sup> Department of Chemistry, Moscow State University, Leninskie Gory 1–3, Moscow 119991, Russia

<sup>c</sup> Institute of Organic Chemistry, Karlsruhe Institute of Technology, Fritz-Haber-Weg 6, Karlsruhe 76131, Germany

<sup>d</sup> DVGW Research Center for Water Chemistry and Water Technology, Karlsruhe Institute of Technology, Engler-Bunte-Ring 9, Karlsruhe 76131, Germany

## ARTICLE INFO

### Article history:

Received 17 June 2015

Received in revised form 9 September 2015

Accepted 18 September 2015

Available online 21 September 2015

### Keywords:

TiO<sub>2</sub>

Photocatalysis

Mechanism

OH radicals

Isotope labeling

## ABSTRACT

In this work, the photocatalytic generation of free OH radicals ( $\bullet\text{OH}_{\text{free}}$ ) in aqueous TiO<sub>2</sub> suspensions was studied using an <sup>18</sup>O isotope labeling and a “remote” photocatalysis approach. A probe compound, 1,3,5-trichlorobenzene (TCB), was adsorbed in pores of silica gel (SG) microparticles and, by this, was shielded from the direct hole oxidation. Penetration of the TiO<sub>2</sub> particles (25 nm in size) to the TCB, adsorbed in the SG pores, was blocked due to a small size of the SG pores (4 nm). Therefore, the “remote” degradation of the TCB was solely driven by  $\bullet\text{OH}_{\text{free}}$ , and this allowed us to selectively determine the quantum yield of the  $\bullet\text{OH}_{\text{free}}$  generation. The isotope labeling with <sup>18</sup>O has demonstrated that the major pathway of the  $\bullet\text{OH}_{\text{free}}$  formation is the direct hole oxidation of H<sub>2</sub>O, whereas the reduction of dissolved O<sub>2</sub> by photogenerated electrons contributes in less than 5% of the total amount of  $\bullet\text{OH}_{\text{free}}$ . Nevertheless, the latter pathway becomes more important if holes are scavenged. This work sheds light on the intrinsic roles of photogenerated holes and electrons in the mechanism of the  $\bullet\text{OH}_{\text{free}}$  formation in aqueous TiO<sub>2</sub> photocatalysis.

© 2015 Elsevier B.V. All rights reserved.

## 1. Introduction

UV-illumination of aqueous suspensions of TiO<sub>2</sub> results in the generation of electron–hole ( $e^-$ – $h^+$ ) pairs in the TiO<sub>2</sub> crystals and in the formation of reactive oxygen species (ROS) at the TiO<sub>2</sub>/H<sub>2</sub>O interface [1]. If  $h^+$  and  $e^-$  are localized at the TiO<sub>2</sub> surface (more rigorously, at the bands of the TiO<sub>2</sub> surface slab), they can induce redox reactions with constituents of the solution. The direct reaction of  $h^+$  with adsorbed species (e.g., organic contaminants) results in the oxidation of the species via direct electron transfer. At the same time, the reaction of  $h^+$  with H<sub>2</sub>O (either physisorbed or chemisorbed) and the reaction of  $e^-$  with dissolved O<sub>2</sub> result in the formation of free  $\bullet\text{OH}$  ( $\bullet\text{OH}_{\text{free}}$ ). Those  $h^+$  that are conjugated with surface titanol groups in a form of electron deficient  $>\text{Ti}-\text{OH}^+$  can be considered as surface bound  $\bullet\text{OH}$  ( $\bullet\text{OH}_{\text{surf}}$ ) [2].

\* Corresponding author at: Institute of Nanotechnology, Karlsruhe Institute of Technology, Hermann-von-Helmholtz-Platz 1, 76344, Eggenstein-Leopoldshafen, Germany. Fax: +49 721 608 47051.

E-mail addresses: [aleksandr.kondrakov@kit.edu](mailto:aleksandr.kondrakov@kit.edu), [alexander.kondrakov@gmail.com](mailto:alexander.kondrakov@gmail.com) (A.O. Kondrakov).

It is generally supposed that  $h^+$  or  $\bullet\text{OH}_{\text{surf}}$  (hereafter, also  $h^+$ ) react with adsorbed species via direct electron transfer, whereas mobile  $\bullet\text{OH}_{\text{free}}$  typically participate in  $\bullet\text{OH}$ -addition or hydrogen abstraction reactions in solution bulk [3–6]. For example, the  $h^+$ -driven oxidation of bisphenol A during its photocatalytic degradation produces genotoxic quinone-like products, whereas the  $\bullet\text{OH}_{\text{free}}$  addition results in the formation of much less harmful catechols [7]. The role of the direct  $h^+$ -driven oxidation of a contaminant depends on its affinity to the TiO<sub>2</sub> surface. At the same time, the photocatalytic oxidation by mobile  $\bullet\text{OH}_{\text{free}}$  represents an opposite case: it is an unselective, omnipresent reaction [8,9], which occurs at the TiO<sub>2</sub>/H<sub>2</sub>O interface and also in the solution bulk.

Current reports on predominance of one or another pathway of the  $\bullet\text{OH}_{\text{free}}$  generation (the oxidation of H<sub>2</sub>O by  $h^+$  or the reduction of dissolved O<sub>2</sub> by  $e^-$ ) as well as the data on  $\bullet\text{OH}_{\text{free}}$  generation quantum yields are controversial [10–15]. As a consequence, the mechanism of the  $\bullet\text{OH}_{\text{free}}$  formation remains under debate and the fundamental understanding of aqueous TiO<sub>2</sub> photocatalysis is not consistent [2,4,16,17]. Therefore, further investigations on the  $\bullet\text{OH}_{\text{free}}$  formation chemistry are highly important.

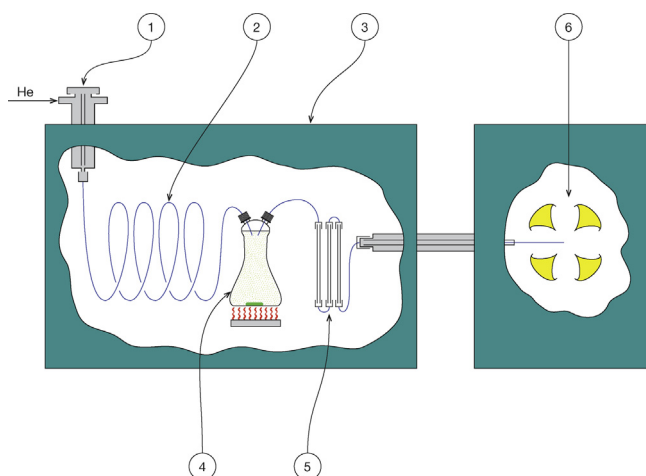


**Fig. 1.** GC–MS setup developed for monitoring of TCB adsorption in SG pores: (1) GC inlet with flow controller, (2) 5 m × 0.32 mm deactivated silica capillary, (3) GC oven, (4) gas-tight flask with solid TCB, (5) SG particles packed in multiple columns, (6) quadrupole mass-analyzer.

This work aims at the identification of precursors and the estimation of amounts of photocatalytically generated  $\bullet\text{OH}_{\text{free}}$ . The identification of the  $\bullet\text{OH}_{\text{free}}$  precursors was performed in isotope-labeling experiments using  $^{18}\text{O}_2$  dissolved in  $\text{H}_2^{16}\text{O}$ . The specific roles of  $e^-$  and  $h^+$  in the  $\bullet\text{OH}_{\text{free}}$  generation were investigated using scavenging effects of  $\text{Ag}^+$ ,  $\text{HCOOH}$  and tert-butanol (tBuOH). To selectively explore  $\bullet\text{OH}_{\text{free}}$ , we adsorbed 1,3,5-trichlorobenzene (TCB) in pores of silica gel (SG) microparticles and monitored kinetics of its “remote” photocatalytic degradation. Due to the structural symmetry of TCB molecule, the reaction with  $\bullet\text{OH}_{\text{free}}$  transforms TCB solely to the single degradation product, 2,4,6-trichlorophenol (TCP) [18]. In mixed suspensions of  $\text{TiO}_2$  and SG, the small diameter ( $d = 4 \text{ nm}$ ) of the SG pores prevents penetration of the  $\text{TiO}_2$  particles ( $d = 25 \text{ nm}$ ) to the adsorbed TCB. Therefore, the formation of TCP was primarily driven by the reaction of TCB with  $\bullet\text{OH}_{\text{free}}$ , not with  $h^+$  at the  $\text{TiO}_2$  surface.

## 2. Experimental section

### 2.1. Materials

$\text{TiO}_2$  powder AEROXIDE P25 (former Degussa P25) was obtained from Evonik Industries AG, Germany. All  $\text{TiO}_2$  samples were annealed in air at  $300^\circ\text{C}$  for 1 h in order to destruct carbon impurities of the AEROXIDE P25 powder, since they can act as electron donors [19]. TCB (purity 99%), TCP (purity 99%), SG (ultrapure for column chromatography, particle size  $10 \mu\text{m}$  to  $60 \mu\text{m}$ , pore size  $4 \text{ nm}$ ) and phenylglyoxylic acid (purity min. 98%) were obtained from Sigma–Aldrich, Steinheim, Germany. tBuOH (purity min. 99.5%), purchased from VWR, Bruchsal, Germany, was additionally distilled before the experiments.  $\text{AgNO}_3$  (p.a.) was obtained from Merck, Darmstadt, Germany. All organic solvents were of HPLC grade. Ultrapure water, generated by a Purelab flex device (ELGA, Celle, Germany) out of distilled water, was used in all the experiments.

### 2.2. Adsorption of TCB in SG pores

The adsorption of TCB on SG was performed in a column packed with 420 mg of the SG particles and installed in a GC–MS system (Fig. 1). He carrier gas from a GC inlet (1), after passing through a silica capillary (2), was saturated with TCB vapor (4) and then passed through a cascade of the SG columns (5), whose outlet was con-

nected to an MS detector (6). Solid TCB was evaporated in a gas-tight flask (4), thermostated at  $80^\circ\text{C}$  in a GC oven (3). The TCB vapor was continuously pumped by the He flow ( $v = 1.6 \text{ mL min}^{-1}$ ) to the SG columns, where TCB was adsorbed. The adsorption rate was monitored by the MS detector at  $m/z$  145. The MS parameters were identical to those set in subsequent GC–MS measurements. The intensity of the MS signal of TCB obtained with an empty column (without the SG phase) was used as the indicator of saturation of the SG columns by TCB. When the TCB breakthrough was observed on the same level as for the empty column, the adsorption process was terminated by closing a connection between the SG columns and the evaporation flask.

### 2.3. Photocatalytic degradation

A solar simulator Oriel Sol 3A (Newport Corp., Stratford, CT, USA) was used as the source of UVA light. The intensity of the polychromatic UVA light, generated by the solar simulator, was equal to  $I_0 = 5 \mu\text{E s}^{-1}$ , measured by a phenylglyoxylic acid actinometer as described elsewhere [20,21]. All the solutions of phenylglyoxylic acid were prepared directly before measurements.

In all the experiments, the  $\text{TiO}_2$  and SG loads were  $0.1 \text{ g L}^{-1}$  and  $4 \text{ g L}^{-1}$ , respectively. Before each experiment,  $\text{TiO}_2$  suspensions were ultrasonicated for 30 min, mixed with scavengers (the concentrations:  $c(\text{Ag}^+) = 2 \text{ mM}$ ,  $c(\text{HCOOH}) = 45 \text{ mM}$  and  $c(\text{tBuOH}) = 54 \text{ mM}$  were chosen according to previous studies [8,22,23]) and kept in dark for 30 min to reach adsorption equilibria. Then SG particles with adsorbed TCB were added. During the degradation experiments, the samples were thermostated at  $20^\circ\text{C}$  in a water bath filled with circulating water. A continuous mixing with a magnetic stirrer prevented sedimentation of  $\text{TiO}_2$  and SG particles. The irradiation path length was kept constant at  $l = 4 \text{ cm}$  in all the experiments. The suspensions were not buffered to avoid an influence of inorganic constituents. A preliminary experiment in a non-buffered medium (with the initial pH 6.7) showed no significant change in pH throughout the reaction. Therefore, all further experiments were conducted without pH control. All the degradation experiments were conducted in triplicate, and the obtained data were averaged.

### 2.4. Isotope labeling experiments

In the experiments with  $^{18}\text{O}_2$ , the samples were prepared in a glovebox with  $\text{N}_2$  atmosphere (the residual aerial  $\text{O}_2$  content was about 3 ppm). The concentration of dissolved  $\text{O}_2$  was measured by a fluorescence sensor FDO 701 IQ SW (WTW, Germany). The ultrapure water used for the preparation of  $\text{TiO}_2$  suspensions was purged by  $\text{N}_2$  until the concentration of dissolved  $^{16}\text{O}_2$  became lower  $0.1 \text{ mg L}^{-1}$  and then by  $^{18}\text{O}_2$  until the concentration of dissolved  $^{18}\text{O}_2$  reached  $9 \text{ mg L}^{-1}$  (the equilibrium concentration of  $\text{O}_2$  dissolved in water under the atmospheric pressure at the room temperature). The mixed suspensions of  $\text{TiO}_2$  and SG with TCB adsorbed in the SG pores were prepared by addition of the certain amounts of dry SG powder (with TCB adsorbed under a flow of ultrapure He as described above) and  $\text{TiO}_2$  powder to  $^{18}\text{O}_2$ -rich water aliquots. The samples were isolated from the atmosphere by gas-tight caps with quartz windows. The irradiation of the samples was conducted under the conditions described in Section 2.3.

### 2.5. Methods of analysis

The method of dispersive liquid microextraction (DLME) [24] was adopted for an one-step extraction of TCB and its degradation product, TCP. The samples were extracted by a cloudy solution formed of dichloromethane mixed with acetone in the volumetric ratio of 5:1. Further details on the recovery and the reproducibility

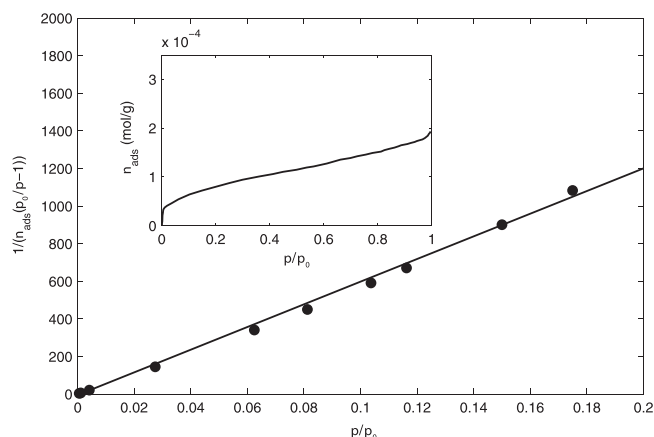


Fig. 2. BET isotherm for the adsorption of TCB in SG pores. The inset shows the TCB adsorption isotherm in the mesoporous region.

of the developed DLME procedure are given in Supplementary data Table S1.

The GC–MS analysis was carried out using a gas chromatograph Agilent 7890A equipped with a split/splitless injector, a mass spectrometer Agilent 5975 and an analytical column HP-5MS 30 m × 0.32 mm × 0.25 μm (Agilent Technologies, Waldbronn, Germany). Samples, of 1 μL volume, were injected in a splitless mode at 200 °C. The flow rate of He carrier gas was  $\nu = 1.6 \text{ mL min}^{-1}$ . The GC oven program was 45 °C (3 min) – 20 °C/min – 240 °C (4 min). The mass spectra were obtained in an electron impact ionization mode at 70 eV. The MS fragments at  $m/z$  145, 196 and 198 were used for the quantification of TCB, TCP and TCP containing  $^{18}\text{O}$ -atoms (TCP- $^{18}\text{O}$ ), respectively.

### 3. Results and discussion

#### 3.1. Adsorptive behavior of TCB in SG pores

The TCB adsorption in the SG pores was monitored by the MS detector of the GC–MS system. The quantity of TCB adsorbed at a given time  $t$  was calculated according to Eq. (1).

$$n_{\text{ads}} = \frac{q_{\text{max}} m_{\text{SG}}}{M_{\text{TCB}}} \frac{I_t}{I_{\text{max}}} \quad (1)$$

where  $n_{\text{ads}}$  is the amount of adsorbed TCB (mol);  $q_{\text{max}}$  is the maximum mass of TCB adsorbed per the mass of the SG phase ( $\text{g g}^{-1}$ );  $m_{\text{SG}}$  is the mass of the SG phase (g);  $M_{\text{TCB}}$  is the molar mass of TCB ( $\text{g mol}^{-1}$ );  $I_t$  and  $I_{\text{max}}$  are the momentary and maximal TCB signals of the MS detector at  $m/z$  145. Taking the reciprocal of  $I_t/I_{\text{max}}$  equal to the relative TCB pressure ( $p/p_0$ ), one obtains a BET equation (Eq. (2)).

$$\left(n_{\text{ads}} \left(\frac{p_0}{p} - 1\right)\right)^{-1} = \frac{c-1}{n_m c} \frac{p}{p_0} + \frac{1}{n_m c} \quad (2)$$

where  $c$  is a BET constant;  $n_m$  is the amount of monolayer adsorbed TCB per the mass of the SG phase ( $\text{mol g}^{-1}$ ).

Further, an adsorption BET isotherm in the form of  $(n_{\text{ads}} (p_0/p - 1))^{-1}$  vs.  $p/p_0$  can be plotted (Fig. 2).

A linearity of the BET isotherm in the  $p/p_0$  range from 0.0 to 0.2 corresponds to the formation of a TCB monolayer within the range. To calculate the adsorption site area,  $A_{\text{BET}}$ , we divide the known BET surface area,  $S_{\text{BET}}$ , of the SG [25] by the number,  $n_m N_A$ , of TCB molecules constituting the monolayer (Eq. (3)).

$$A_{\text{BET}} = \frac{S_{\text{BET}}}{n_m N_A} \quad (3)$$

where  $N_A$  is Avogadro's number.

Table 1

Parameters of the TCB adsorption in SG pores.

Parameter	Value
$n_m, \text{mol g}^{-1}$	$0.75 \times 10^{-4}$
$R^2$	0.9983
$A_{\text{BET}}, \text{nm}^2$	8.8
$A_{\text{TCB}}, \text{nm}^2$	1.4

At the same time, the maximal area,  $A_{\text{TCB}}$ , occupied by a single symmetric TCB molecule can be estimated on the basis of the lengths and the angles of the TCB bonds [26]:

$$A_{\text{TCB}} = 3 \sin \frac{\alpha}{2} (l_{\text{CC}} + l_{\text{CCl}})(l_{\text{CC}} + l_{\text{CH}}) \quad (4)$$

where  $\alpha$  is the internal angle between two adjacent CC bonds in TCB molecule;  $l_{\text{CC}}$ ,  $l_{\text{CCl}}$  and  $l_{\text{CH}}$  are the lengths of the C–, C–Cl and C–H bonds in TCB molecule (Supplementary data Fig. S1).

The estimated values of  $n_m$ ,  $A_{\text{BET}}$  and  $A_{\text{TCB}}$  are given in Table 1. The fact that  $A_{\text{BET}} > A_{\text{TCB}}$  argues for a loose structure of the TCB adsorption layer. Moreover, a comparison of the GS-MS monitoring and the BET analysis showed that 40% of the total amount of adsorbed TCB constituted a monolayer.

Analysis of a SG suspension supernatant revealed a negligible (<5%) migration of TCB from the SG phase to the water phase within 6 h. The total BET area of the SG particles ( $>400 \text{ m}^2 \text{ g}^{-1}$  [25]) is significantly larger than their external surface area (which varies from 0.07 to  $0.4 \text{ m}^2 \text{ g}^{-1}$  for spherical particles with the diameters from 60 to 10 μm, respectively). Therefore, the amount of TCB adsorbed in the SG pores was significantly larger than the fraction of TCB adsorbed at the outer surface of the SG particles (the latter constituted less than 1% of the total amount of adsorbed TCB). Taken together, these data show that the major part of TCB was strongly bound inside the SG pores and was available for the attack of diffusive  $\bullet\text{OH}_{\text{free}}$ .

#### 3.2. Reactions of $\bullet\text{OH}_{\text{free}}$ in SG pores

Previous reports on the dual  $\text{h}^+/\bullet\text{OH}_{\text{free}}$ -mechanism of the photocatalytic degradation of organic compounds are rather tentative in respect to specific roles of  $\bullet\text{OH}_{\text{free}}$  and  $\text{h}^+$  [8,27–29]. Herein, we have developed a new approach of “remote” photocatalysis, where adsorbed TCB served as a probe compound for the selective detection of  $\bullet\text{OH}_{\text{free}}$ . The  $\text{h}^+$ -driven degradation, common for aromatic compounds [30], was ruled out, because the adsorbed TCB was shielded in the SG pores from the reaction with  $\text{h}^+$ .

Once we ensured that TCB was strongly retained in the SG pores, any contact between the TCB and the  $\text{TiO}_2$  became highly unlikely. The smallness of the SG pores ( $d = 4 \text{ nm}$ ) prevents penetration of the  $\text{TiO}_2$  particles ( $d = 25 \text{ nm}$ ) to the adsorbed TCB. The amount of TCB adsorbed at the outer surface of the SG microparticles was neglected, because the outer surface area is small compared to the total area of the SG pores (respectively,  $<0.4$  and  $>400 \text{ m}^2 \text{ g}^{-1}$  [25]). Analysis of a DLME concentrate obtained from a supernatant of an illuminated mixed suspension of the SG and the  $\text{TiO}_2$  showed that less than 5% of the initial amount of adsorbed TCB migrated into the aqueous phase and was oxidized there. The migration of TCB was limited, particularly, because of its poor solubility in water ( $<1 \text{ ppm}$  [31]). Therefore, the competition for  $\bullet\text{OH}_{\text{free}}$  between dissolved and adsorbed TCB was negligible, and it was assumed that all  $\bullet\text{OH}_{\text{free}}$  reacted only with the adsorbed TCB.

In addition, analysis of control samples (SG suspensions with adsorbed TCB in presence and absence of  $\text{TiO}_2$ ) kept in dark pointed out that there was neither a disappearance of TCB nor a formation of TCP. Taking into account the considerations above, we conclude that the transformation of TCB to TCP in the SG pores was solely driven by  $\bullet\text{OH}_{\text{free}}$ .

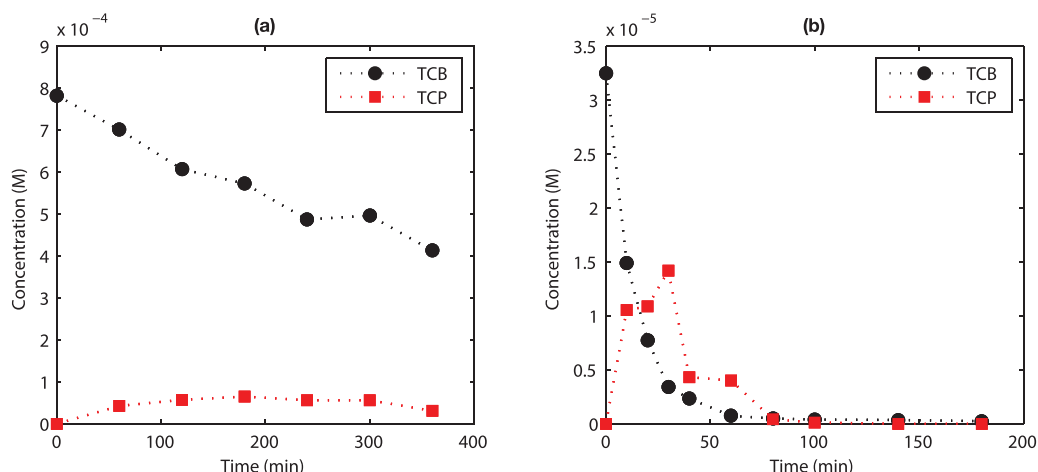


**Fig. 3.** Photocatalytic degradation of TCB and formation of TCP in (a) SG pores and (b) a  $\text{TiO}_2$  suspension.  $\rho(\text{TiO}_2) = 0.1 \text{ g L}^{-1}$ ,  $\rho(\text{SG}) = 4 \text{ g L}^{-1}$ ,  $I_0 = 5 \mu\text{E s}^{-1}$ ,  $T = 25^\circ\text{C}$ .

**Table 2**

Kinetics parameters of the TCP formation out of TCB adsorbed in SG pores and dissolved in a  $\text{TiO}_2$  suspension.

Parameter	Value	
	SG pore	$\text{TiO}_2$ suspension bulk
$k, \text{s}^{-1}$	$3.5 \times 10^{-5}$	$8.9 \times 10^{-4}$
$n$	1	1
$\nu_{\text{TCP}}$	0.5	1
$\Phi$	0.002	0.04

The degradation of TCB adsorbed in the SG pores (Fig. 3a) exhibited a different stoichiometry compared to a control experiment on the degradation of TCB dissolved in a  $\text{TiO}_2$  suspension without SG (Fig. 3b). In particular, the stoichiometric coefficient,  $\nu_{\text{TCP}}$  estimated by Eq. (5), of the TCP formation in the SG pores was significantly lower than that obtained for the formation of TCP in the  $\text{TiO}_2$  suspension (Table 2).

$$\nu_{\text{TCP}} = \frac{c_t(\text{TCP})}{\Delta_t \xi} \quad (5)$$

where  $c_t(\text{TCP})$  is the concentration of TCP formed up to a given time  $t$  (M);  $\Delta_t \xi = \Delta c(\text{TCB})/n$  is the extent of reaction up to the time  $t$  (M), assuming that the reaction order  $n = 1$ .

The data in Table 2 demonstrate a difference between the reaction order and the stoichiometry. Such variations are typical for reactions occurring under dimensional constraints [32]. Today, there is no consensus on a kinetic formalism for reactions in porous media. Therefore, the quantum yield,  $\Phi_{\text{OH}}$ , of the  $\bullet\text{OH}_{\text{free}}$  generation was estimated using the classical homogeneous kinetics, assuming that

$$\Phi_{\text{OH}} = \Phi_{\text{pore}} = \frac{k_{\text{pore}}}{k_{\text{bulk}}} \Phi_{\text{bulk}} \quad (6)$$

where  $\Phi_{\text{pore}}$  and  $k_{\text{pore}}$  are, respectively, the quantum yield and the apparent first-order rate constant of the photocatalytic degradation of TCB adsorbed in the SG pores;  $\Phi_{\text{bulk}}$  and  $k_{\text{bulk}}$  are, respectively, the quantum yield and the apparent first-order rate constant of the photocatalytic degradation of TCB dissolved in the  $\text{TiO}_2$  suspension without SG.

In turn,  $\Phi_{\text{bulk}}$  can be calculated by Eq. (7)

$$\Phi_{\text{bulk}} = \frac{dn(\text{TCB})}{dt} I_{\text{abs}}^{-1} \quad (7)$$

where  $\frac{dn(\text{TCB})}{dt}$  is the rate of the photocatalytic degradation of TCB dissolved in the  $\text{TiO}_2$  suspension ( $\text{mol s}^{-1}$ );  $I_{\text{abs}}$  is the UVA (300 nm to 380 nm) photon flux ( $\text{E s}^{-1}$ ).  $I_{\text{abs}}$  was determined by a chemical

actinometry, assuming that UVA light was completely absorbed by the  $\text{TiO}_2$  suspension along the 4 cm light path.

A comparison of the  $\Phi_{\text{pore}}$  and  $\Phi_{\text{bulk}}$  values (Table 2) indicates that  $\bullet\text{OH}_{\text{free}}$  reacted in the SG pores constituted a 5% fraction of the total amount of photogenerated  $\bullet\text{OH}$  (which include both the surface  $\text{h}^+$  and mobile  $\bullet\text{OH}_{\text{free}}$ ). In this way,  $\Phi_{\text{OH}} = 0.002$ .

It should be noted that the bimolecular self-recombination of  $\bullet\text{OH}_{\text{free}}$  forms  $\text{H}_2\text{O}_2$  [12]. However, this process becomes important only if the concentration of  $\bullet\text{OH}_{\text{free}}$  is comparable or higher than the concentration of a substrate (in our case TCB), or if the reactivity of  $\bullet\text{OH}_{\text{free}}$  towards the substrate is low [33]. Under the conditions applied herein, the rate of the  $\bullet\text{OH}_{\text{free}}$  self-recombination is much lower than the rate of the reaction between  $\bullet\text{OH}_{\text{free}}$  and TCB, and  $\bullet\text{OH}_{\text{free}}$  diffusion limitations can be excluded (Supplementary data Notes S1 and S2). And since  $\text{Si}^{\text{IV}}\text{-OH}$  and  $\text{Si}^{\text{IV}}\text{-O}^-$  groups of the SG are highly stable and hardly react with  $\bullet\text{OH}_{\text{free}}$ , we assume that  $\bullet\text{OH}_{\text{free}}$  reacted only with the adsorbed TCB, not with other constituents of the suspension.

At ambient temperatures,  $\bullet\text{OH}_{\text{free}}$ -adducts of benzenes preferably stabilize to hydroxycyclohexadienyl radicals, making the H-abstraction unfavorable [34]. Therefore, we consider that the  $\bullet\text{OH}_{\text{free}}$  attack leads to the TCB hydroxylation. The cooperative mesomeric effect of the three TCB chloro-groups activates ortho and para positions for the  $\bullet\text{OH}_{\text{free}}$ -attack [35], resulting in the sole formation of TCP. GC–MS chromatograms of probes, sampled throughout the reaction, showed negligible formation of by-products other than TCP (dichlorophenols, chloroquinones, etc.). It indicates that TCB is a suitable probe compound for the determination of  $\bullet\text{OH}_{\text{free}}$ , since the transformation of TCB to TCP is not heavily accompanied by competing side-reactions.

Nevertheless, the dimensional constraints and, possibly, a competing reaction between diffusing  $\bullet\text{OH}_{\text{free}}$  and TCP, continuously forming during the reaction, resulted in the stoichiometry deviations, which do not allow us to unambiguously equal the molar amount of degraded TCB to that of generated  $\bullet\text{OH}_{\text{free}}$ . Therefore, we consider the estimated value of  $\Phi_{\text{OH}}$  as the lower bound for the “true” value of the quantum yield of the  $\bullet\text{OH}_{\text{free}}$  generation. In other words, we consider that  $\bullet\text{OH}_{\text{free}}$  constituted at least 5% of the total amount of photocatalytically generated  $\bullet\text{OH}$ .

### 3.3. Effects of scavengers on $\bullet\text{OH}_{\text{free}}$ generation efficiency

While  $\bullet\text{OH}_{\text{surf}}$  are defined as  $\text{h}^+$  conjugated with surface titanol groups in a form of electron deficient  $>\text{Ti-OH}^+$  [4], a predominant pathway of the  $\bullet\text{OH}_{\text{free}}$  formation is questionable [2,16]. Although  $\text{H}_2\text{O}$  is considered to be the primary precursor of  $\bullet\text{OH}_{\text{free}}$  [12], the

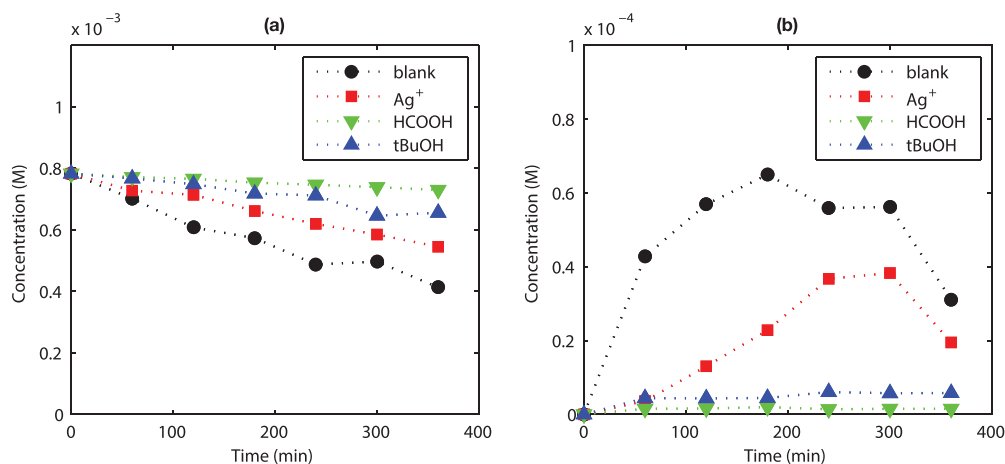


**Fig. 4.** (a) Photocatalytic degradation of TCB and (b) formation of TCP in SG pores in presence of  $\text{Ag}^+$ ,  $\text{HCOOH}$  and  $\text{tBuOH}$ .  $\rho(\text{TiO}_2) = 0.1 \text{ g L}^{-1}$ ,  $\rho(\text{SG}) = 4 \text{ g L}^{-1}$ ,  $c(\text{Ag}^+) = 2 \text{ mM}$ ,  $c(\text{HCOOH}) = 45 \text{ mM}$ ,  $c(\text{tBuOH}) = 54 \text{ mM}$ ,  $I_0 = 5 \mu\text{E s}^{-1}$ ,  $T = 25^\circ\text{C}$ .

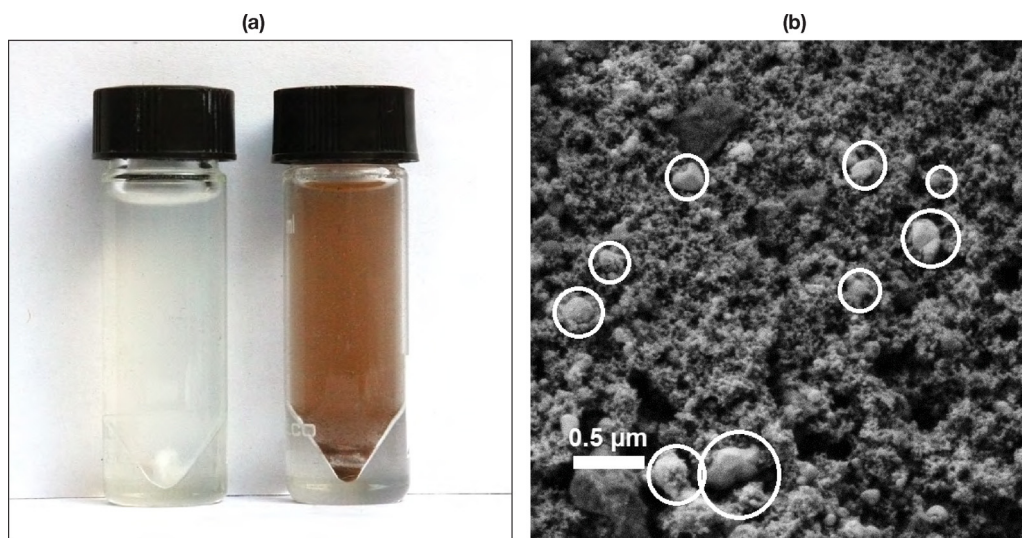


**Fig. 5.** (a) Color of a SG-TiO<sub>2</sub> suspension before (on the left) and after (on the right) an 1 h photocatalytic treatment in presence of 2 mM  $\text{Ag}^+$ . (b) SEM micrograph illustrating deposition of  $\text{Ag}^0$  particles on the TiO<sub>2</sub>, the largest particles are marked by the circles. The experimental conditions are the same as those given in Fig. 3.

formation of  $\bullet\text{OH}_{\text{free}}$  out of dissolved  $\text{O}_2$  has not been denied by now [23].  $\bullet\text{OH}_{\text{free}}$  can be generated via the reduction of dissolved  $\text{O}_2$  by photogenerated  $e^-$  followed by the dismutation or the further reduction of  $\text{O}_2^{\bullet-}$  [36]. The formation of  $\bullet\text{OH}_{\text{free}}$  out of  $\text{H}_2\text{O}$  occurs, in turn, via the  $h^+$ -driven oxidation. By now, the specific roles of these two pathways ( $e^-$  and  $h^+$ -mediated) are not clear [10,23]. To assess their contributions to the  $\bullet\text{OH}_{\text{free}}$  generation, we investigated the influence of scavengers on the degradation of TCB adsorbed in pores of the SG. Herein,  $\text{Ag}^+$ ,  $\text{HCOOH}$  and  $\text{tBuOH}$  were used as the scavengers for  $e^-$ ,  $h^+$  and  $\bullet\text{OH}_{\text{free}}$ , respectively [23,37]. The optimal concentrations of the scavengers were chosen on the basis of their selective inhibition effects reported previously [5,8,23,38].

Experimental concentration profiles of the photocatalytic degradation of TCB and the formation of TCP in the presence of  $\text{Ag}^+$ ,  $\text{HCOOH}$  and  $\text{tBuOH}$  are shown in Fig. 4a and b. A decrease in the TCP formation rate occurred in the presence of  $\text{tBuOH}$  and  $\text{HCOOH}$  is attributed to the scavenging of, respectively,  $\bullet\text{OH}_{\text{free}}$  and those  $h^+$  that serve as the  $\bullet\text{OH}_{\text{free}}$  precursors [23].

The effect of  $\text{Ag}^+$  was dual. On the one hand, the reaction between  $\text{Ag}^+$  and  $e^-$  can suppress the production of  $\bullet\text{OH}_{\text{free}}$  via the  $e^-$ -mediated reduction of dissolved  $\text{O}_2$  on the TiO<sub>2</sub> surface [37]. It should be noted, that the maximal coverage of the TiO<sub>2</sub>

surface by  $\text{Ag}^+$  was achieved throughout the reaction due to a significant excess of  $\text{Ag}^+$ . The initial amount of  $\text{Ag}^+$  ( $n(\text{Ag}^+) = 20 \mu\text{mol}$ ) exceeded the maximum TiO<sub>2</sub> capacity for the adsorption of  $\text{Ag}^+$  ( $n(\text{Ag}^+)_{\text{max}} = 15 \text{ nmol}$  [39] for  $\rho(\text{TiO}_2) = 1 \text{ mg}$ ) by several orders of magnitude. A kinetics analysis shows that under the applied conditions the reduction of  $\text{Ag}^+$  proceeds much faster than the reduction of  $\text{O}_2$  (Supplementary data Note S3).

The  $\text{Ag}^+$  counter ion,  $\text{NO}_3^-$ , slowly reacts with  $\bullet\text{OH}$  ( $k = 2.8 \times 10^5 \text{ M}^{-1} \text{ s}^{-1}$  [40]). Therefore, at the concentration used it did not compete with TCB for  $\bullet\text{OH}_{\text{free}}$  nor  $h^+$ . On the other hand, the photocatalytic reduction of  $\text{Ag}^+$  leads to the deposition of  $\text{Ag}^0$  on the TiO<sub>2</sub> surface and, by this, decreases efficiency of the light absorption by the TiO<sub>2</sub> [37]. Within the first hour of the reaction, the TiO<sub>2</sub> suspension gradually became brown (Fig. 5a). The SEM micrographs (Fig. 5b) together with the results of EDX analysis (Supplementary data Fig. S2) show that relatively large ( $d = 50 \text{ nm}$  to  $300 \text{ nm}$ ) particles of  $\text{Ag}^0$  were formed in the suspension. Nevertheless, Fig. 4a demonstrates that the presence of  $\text{Ag}^+$  only partially retarded the degradation of TCB adsorbed in the SG pores. It implies that the trapping of  $e^-$  by  $\text{Ag}^0$  particles deposited on the TiO<sub>2</sub> surface can suppress the  $e^-$ - $h^+$  recombination [41] and maintain the  $h^+$  concentration on a level that is sufficient for the formation of  $\bullet\text{OH}_{\text{free}}$  out of  $\text{H}_2\text{O}$ .

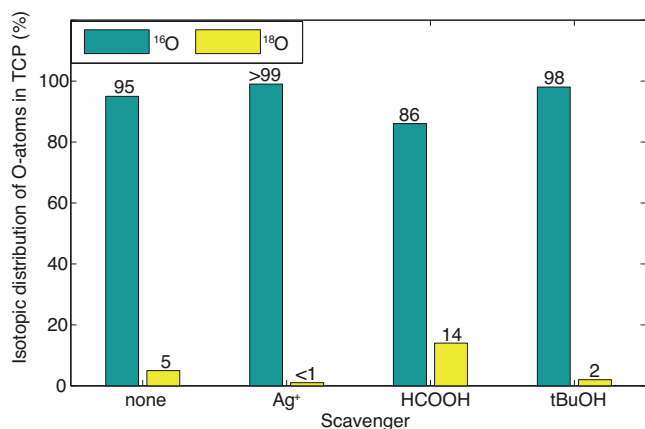


**Fig. 6.** Effects of  $\text{Ag}^+$ , HCOOH and tBuOH on the isotopic distribution of O-atoms in TCP formed in the presence of  $^{18}\text{O}_2$  dissolved in  $\text{H}_2^{16}\text{O}$ .  $\rho(\text{TCB}) = 142 \text{ mg L}^{-1}$ ,  $\rho(\text{TiO}_2) = 0.1 \text{ g L}^{-1}$ ,  $\rho(\text{SG}) = 4.0 \text{ g L}^{-1}$ ,  $c(^{18}\text{O}_2) = 0.28 \text{ mM}$ ,  $I_0 = 5 \text{ mW cm}^{-2}$ , irradiation time 6 h, pH 7,  $T = 25^\circ\text{C}$ .

Taken together, our results suggest that the rate of the  $\bullet\text{OH}_{\text{free}}$ -driven degradation of TCB adsorbed in the SG pores strongly depends on the  $\text{h}^+$  concentration. It supports the hypothesis on the predominance of the  $\text{h}^+$ -driven pathway of the  $\bullet\text{OH}_{\text{free}}$  generation.

### 3.4. Isotopic distribution of O-atoms in $\bullet\text{OH}_{\text{free}}$

To further clarify the specific roles of  $\text{H}_2\text{O}$  and dissolved  $\text{O}_2$  as  $\bullet\text{OH}_{\text{free}}$  precursors, we conducted the photocatalytic degradation of TCB in presence of dissolved  $^{18}\text{O}_2$ . The TCB was adsorbed in pores of the SG particles which were then suspended together with the  $\text{TiO}_2$  in  $\text{H}_2^{16}\text{O}$  enriched with  $^{18}\text{O}_2$  (up to the concentration of  $9 \text{ mg L}^{-1}$ ). Isotopic distribution of O-atoms in the formed TCP was determined on the basis of the  $m/z$  signals for the molecular ion of TCP obtained by GC–MS analysis. Further, we investigated the influence of scavengers for  $\text{e}^-$ ,  $\text{h}^+$  and  $\bullet\text{OH}_{\text{free}}$  (respectively,  $\text{Ag}^+$ , HCOOH and tBuOH) on the isotopic distribution of the TCP O-atoms. Since the oxygen isotope exchange rates between phenol, water and molecular oxygen are negligibly slow [30,42], we suppose that  $^{16}\text{O}$ - and  $^{18}\text{O}$ -atoms in the formed TCP were delivered from  $\bullet\text{OH}_{\text{free}}$  generated out of  $\text{H}_2^{16}\text{O}$  and dissolved  $^{18}\text{O}_2$ , respectively. We have also neglected the photoinduced ( $\text{h}^+$ -driven) isotope exchange between the  $\text{TiO}_2$  surface and dissolved  $^{18}\text{O}_2$ , because at low concentrations (in our case, it was  $0.28 \text{ mM}$ )  $^{18}\text{O}_2$  cannot compete with adsorbed  $\text{H}_2\text{O}$  for  $\text{h}^+$  [43].

An experiment without the scavengers demonstrated a low (5%) abundance of  $^{18}\text{O}$ -atoms in the formed TCP (Fig. 6). Apparently, dissolved  $\text{O}_2$  serves as a minor  $\bullet\text{OH}_{\text{free}}$  precursor. The low contribution of  $^{18}\text{O}_2$  can be explained mechanistically: the reduction of  $\text{O}_2$  by  $\text{e}^-$  is a complex and relatively slow 3-electron process involving protonation [44], whereas the direct oxidation of  $\text{H}_2\text{O}$  by  $\text{h}^+$  is a fast one-electron process [8]. Besides, the concentration of  $\text{H}_2\text{O}$  (as the solvent) is much higher than that of dissolved  $\text{O}_2$ . Therefore, the rate of the  $\bullet\text{OH}_{\text{free}}$  generation rate via the  $\text{h}^+$ -driven oxidation of  $\text{H}_2\text{O}$  can be significantly higher than the rate of the  $\bullet\text{OH}_{\text{free}}$  formation via the  $\text{e}^-$ -mediated reduction of  $\text{O}_2$ .

Fig. 6 depicts scavenging effects of  $\text{Ag}^+$ , HCOOH and tBuOH on the isotopic distribution of O-atoms in the formed TCP. Although the scavengers significantly retarded the reaction, the stoichiometry of the transformation of TCB to TCP retained the same as for the degradation without the scavengers. Moreover, no additional by-products of the TCB degradation were detected by the GC–MS analysis. On this basis, we assume that the transformation of TCB to TCP in the SG pores proceeded via the same mechanism of the  $\bullet\text{OH}_{\text{free}}$  attack as discussed above. Thus, we consider the isotopic

distribution of O-atoms in TCP formed in the presence of scavengers as a reliable and decisive indicator of the origin of  $\bullet\text{OH}_{\text{free}}$ .

Poorly adsorbing tBuOH slowly reacts with  $\text{h}^+$  or  $\text{e}^-$  at the  $\text{TiO}_2$  surface [23]. It can lower the total concentration of  $\bullet\text{OH}_{\text{free}}$ , but can suppress neither  $\text{h}^+$ - nor  $\text{e}^-$ -mediated generation of  $\bullet\text{OH}_{\text{free}}$  selectively. On the contrary, HCOOH and  $\text{Ag}^+$  are strongly adsorbing species [22,45] and efficient scavengers for photogenerated  $\text{h}^+$  and  $\text{e}^-$  [4,37]. Fig. 6 shows that the presence of HCOOH and  $\text{Ag}^+$  caused noticeable changes in the isotopic distribution of O-atoms in the TCP towards higher amounts of, respectively,  $^{18}\text{O}$  and  $^{16}\text{O}$  (compared to the experiment without scavengers). In the case of HCOOH, a certain part of  $\text{h}^+$  was scavenged and the formation of  $\bullet\text{OH}_{\text{free}}$  out of  $\text{H}_2\text{O}$  was visibly suppressed. In turn,  $\text{Ag}^+$  scavenged a large fraction of  $\text{e}^-$  and, by this, inhibited the formation of  $\bullet\text{OH}_{\text{free}}$  out of  $\text{O}_2$  via the  $\text{e}^-$ -mediated mechanism.

However, observed in all the isotope experiments, the abundance of  $^{16}\text{O}$  in the formed TCP (Fig. 6) indicates that the  $\text{h}^+$ -mediated pathway of the  $\bullet\text{OH}_{\text{free}}$  generation prevailed over the  $\text{e}^-$ -mediated one even when  $\text{h}^+$  were partially scavenged by HCOOH.

On the basis of these observations we deduce that efficient photocatalytic generation of  $\bullet\text{OH}_{\text{free}}$  requires a high availability of the  $\text{TiO}_2$  surface sites where  $\text{h}^+$  react with  $\text{H}_2\text{O}$ . Such “ideal” conditions for the  $\text{h}^+$ -driven oxidation of  $\text{H}_2\text{O}$  were achieved in our experiments without scavengers: the probe compound was oxidized “remotely”, and only  $\text{O}_2$  and  $\text{H}_2\text{O}$  were present at the  $\text{TiO}_2$  surface (at least, during the initial stage of the reaction). Although it seems to be challenging to achieve a similar situation in practical applications, a high potential of “remote” photocatalytic processes, purely driven by mobile  $\bullet\text{OH}_{\text{free}}$ , should be further explored in more detail.

## 4. Conclusions

The experiments on the degradation of the probe compound, TCB, adsorbed in SG pores allowed us to selectively investigate the mechanism of the photocatalytic formation of  $\bullet\text{OH}_{\text{free}}$  in aqueous suspensions of  $\text{TiO}_2$ . We assume that the strong adsorption of TCB prevented its diffusion towards  $\text{h}^+$  (or  $\bullet\text{OH}_{\text{surf}}$ ) at the  $\text{TiO}_2$  surface during the reaction. Therefore, TCB was shielded from the  $\text{h}^+$  and selectively reacted with  $\bullet\text{OH}_{\text{free}}$ .  $\bullet\text{OH}$ -addition is known to prevail over H-abstraction in degradation of benzene compounds by  $\bullet\text{OH}$ . Thus, we suppose that the  $\bullet\text{OH}_{\text{free}}$  adduct of TCB predominantly stabilized to a hydroxytrichlorocyclohexadienyl radical and then to TCP, which was the sole product of TCB degradation.

With the generation quantum yield of 0.002,  $\bullet\text{OH}_{\text{free}}$  “remotely” oxidized a half of the TCB probe within 6 h of the treatment. The formation of  $\text{H}_2\text{O}_2$  out of  $\bullet\text{OH}_{\text{free}}$  was very low and did not affect the accuracy of the  $\Phi_{\text{OH}}$  estimation. Nevertheless, the stoichiometry deviations, common for dimensionally constrained pore reactions, did not allow us to equal the molar amount of degraded TCB to that of generated  $\bullet\text{OH}_{\text{free}}$ . Therefore, the obtained  $\Phi_{\text{OH}}$  value was interpreted as the lower bound for the “true” value of the quantum yield of the  $\bullet\text{OH}_{\text{free}}$  generation.

The isotope labeling experiments with the use of  $^{18}\text{O}_2$  dissolved in  $\text{H}_2^{16}\text{O}$  have evidenced that the  $\text{h}^+$ -driven oxidation of  $\text{H}_2\text{O}$  is the primary pathway of the  $\bullet\text{OH}_{\text{free}}$  generation (the photoinduced oxygen isotope exchange between  $\text{TiO}_2$  and  $^{18}\text{O}_2$  was neglected). In the absence of  $\text{h}^+$  scavengers, the contribution of dissolved  $\text{O}_2$  in the formation of  $\bullet\text{OH}_{\text{free}}$  was low (5%). Once the  $\text{h}^+$ -driven  $\text{H}_2\text{O}$  oxidation was suppressed by HCOOH, the contribution of  $\text{O}_2$  in the generation of  $\bullet\text{OH}_{\text{free}}$  increased up to 14%, but  $\text{H}_2\text{O}$  still remained the main source of  $\bullet\text{OH}_{\text{free}}$ . It implies that efficiency of the photocatalytic generation of  $\bullet\text{OH}_{\text{free}}$  strongly depends on the availability of surface  $\text{h}^+$  for  $\text{H}_2\text{O}$ , but not on the availability of  $\text{e}^-$  for dissolved  $\text{O}_2$ . Thus, the  $\text{e}^-$  trapping role of  $\text{O}_2$  can be delegated to alterna-

tive  $e^-$  traps (e.g., noble metals) without reducing efficiency of the  $\bullet\text{OH}_{\text{free}}$  formation.

Moreover, since the  $\bullet\text{OH}_{\text{free}}$ -driven oxidation of a contaminant does not require its adsorption, photocatalysts with enhanced generation of  $\bullet\text{OH}_{\text{free}}$  can be more resistant to surface poisoning than conventional ones operating mainly via the  $h^+$ -driven oxidation. However, this conclusion needs an additional experimental validation, and the approach of “remote” photocatalysis seems to be a feasible way to verify or disprove it.

## Acknowledgements

The authors gratefully acknowledge the financial support of state Baden-Württemberg by ZO IV research program “Innovation und Exzellenz: Beherrschung komplexer Systeme”.

## Appendix A. Supplementary data

Supplementary data associated with this article can be found, in the online version, at <http://dx.doi.org/10.1016/j.apcatb.2015.09.038>.

## References

- [1] M.R. Hoffmann, S.T. Martin, W. Choi, D.W. Bahnemann, *Chem. Rev.* 95 (1995) 69–96.
- [2] B. Ohtani, *J. Photochem. Photobiol. C* 11 (2010) 157–178.
- [3] D. Monllor-Satoca, R. Gomez, M. Gonzalez-Hidalgo, P. Salvador, *Catal. Today* 129 (2007) 247–255.
- [4] J.F. Montoya, J.A. Velasquez, P. Salvador, *Appl. Catal. B Environ.* 88 (2009) 50–58.
- [5] D.R. Stapleton, I.K. Konstantinou, D. Mantzavinos, D. Hela, M. Papadaki, *Appl. Catal. B Environ.* 95 (2010) 100–109.
- [6] C.S. Turchi, D.F. Ollis, *J. Catal.* 122 (1990) 178–192.
- [7] A.O. Kondrakov, A.N. Ignatev, F.H. Frimmel, S. Bräse, H. Horn, A.I. Revelsky, *Appl. Catal. B Environ.* 160–161 (2014) 106–114.
- [8] Y. Sun, J.J. Pignatello, *Environ. Sci. Technol.* 29 (1995) 2065–2072.
- [9] C. Minero, G. Mariella, V. Maurino, D. Vione, E. Pelizzetti, *Langmuir* 16 (2000) 8964–8972.
- [10] M.A. Henderson, *Surf. Sci. Rep.* 66 (2011) 185–297.
- [11] N.J.F. Dodd, A.N. Jha, *Photochem. Photobiol.* 87 (2011) 632–640.
- [12] J. Zhang, Y. Nosaka, *J. Phys. Chem. C* 118 (2014) 10824–10832.
- [13] D.C. Hurum, A.G. Agrios, K.A. Gray, T. Rajh, M.C. Thurnauer, *J. Phys. Chem. B* 107 (2003) 4545–4549.
- [14] Y. Nosaka, S. Komori, K. Yawata, T. Hirakawa, A.Y. Nosaka, *Phys. Chem. Chem. Phys.* 5 (2003) 4731–4735.
- [15] Z. Wang, W. Ma, C. Chen, H. Ji, J. Zhao, *Chem. Eng. J.* 170 (2011) 353–362.
- [16] B. Ohtani, *Phys. Chem. Chem. Phys.* 16 (2014) 1788–1797.
- [17] B. Ohtani, O.O. Prieto-Mahaney, D. Li, R. Abe, *J. Photochem. Photobiol. A* 216 (2010) 179–182.
- [18] R.J. Watts, T.M. Haeri-McCarroll, A.L. Teel, *J. Adv. Oxid. Technol.* 11 (2008) 354–361.
- [19] N.N. Rao, S. Dube, *Int. J. Hydrogen Energy* 21 (1996) 95–98.
- [20] A. Defoin, R. Defoin-Straatmann, K. Hildenbrand, E. Bittersmann, D. Kreft, H. Kuhn, *J. Photochem.* 33 (1986) 237–255.
- [21] H. Kuhn, S. Braslavsky, R. Schmidt, *Pure Appl. Chem.* 76 (2004) 2105–2146.
- [22] Q. Sun, Y. Xu, *J. Phys. Chem. C* 114 (2010) 18911–18918.
- [23] Y. Li, B. Wen, C. Yu, C. Chen, H. Ji, W. Ma, J. Zhao, *Chem. A Eur. J.* 18 (2012) 2030–2039.
- [24] M. Rezaee, Y. Assadi, M.-R. Milani Hosseini, E. Aghaee, F. Ahmadi, S. Berijani, *J. Chromatogr. A* 1116 (2006) 1–9.
- [25] P. López-Aranguren, J. Saurina, L. Vega, C. Domingo, *Microporous Mesoporous Mater.* 148 (2012) 15–24.
- [26] M. Dimitriu, L.-M. Ivan, D.-O. Dorohoi, *Rom. J. Phys.* 53 (2008) 79–84.
- [27] C. Minero, G. Mariella, V. Maurino, E. Pelizzetti, *Langmuir* 16 (2000) 2632–2641.
- [28] Y.X. Chen, S.Y. Yang, K. Wang, L.P. Lou, *J. Photochem. Photobiol. A* 172 (2005) 47–54.
- [29] P. Kormali, T. Triantis, D. Dimotikali, A. Hiskia, E. Papaconstantinou, *Appl. Catal. B Environ.* 68 (2006) 139–146.
- [30] T.D. Bui, A. Kimura, S. Ikeda, M. Matsumura, *J. Am. Chem. Soc.* 132 (2010) 8453–8458.
- [31] P. Isnard, S. Lambert, *Chemosphere* 17 (1988) 21–34.
- [32] R. Kopelman, *Science* 241 (1988) 1620–1626.
- [33] T. Wu, G. Liu, J. Zhao, H. Hidaka, N. Serpone, *J. Phys. Chem. B* 103 (1999) 4862–4867.
- [34] I.V. Tokmakov, M.C. Lin, *J. Phys. Chem. A* 106 (2002) 11309–11326.
- [35] W.Z. Tang, C.P. Huang, *Waste Manag.* 15 (1995) 615–622.
- [36] V. Diesen, M. Jonsson, *J. Phys. Chem. C* 118 (2014) 10083–10087.
- [37] H. Kyung, J. Lee, W. Choi, *Environ. Sci. Technol.* 39 (2005) 2376–2382.
- [38] R.R.N. Marques, M.J. Sampaio, P.M. Carrapiço, C.G. Silva, S. Morales-Torres, G. Dražić, J.L. Faria, A.M.T. Silva, *Catal. Today* 209 (2013) 108–115.
- [39] Q. Sun, Y. Xu, *J. Phys. Chem. C* 114 (2010) 18911–18918.
- [40] P.Y. Jiang, Y. Katsumura, K. Ishigure, Y. Yoshida, *Inorg. Chem.* 31 (1992) 5135–5136.
- [41] H.M. Sung-Suh, J.R. Choi, H.J. Hah, S.M. Koo, Y.C. Bae, *J. Photochem. Photobiol. A* 163 (2004) 37–44.
- [42] X. Pang, W. Chang, C. Chen, H. Ji, W. Ma, J. Zhao, *J. Am. Chem. Soc.* 136 (2014) 8714–8721.
- [43] S. Sato, *J. Phys. Chem.* 91 (1987) 2895–2897.
- [44] T. Hirakawa, T. Daimon, M. Kitazawa, N. Ohguri, C. Koga, N. Negishi, S. Matsuzawa, Y. Nosaka, *J. Photochem. Photobiol. A* 190 (2007) 58–68.
- [45] H. Onishi, T. Aruga, Y. Iwasawa, *J. Am. Chem. Soc.* 115 (1993) 10460–10461.